

## MAJOR PAPER

# Influence of Mild White Matter Lesions on Voxel-based Morphometry

Masami Goto<sup>1\*</sup>, Akifumi Hagiwara<sup>2</sup>, Shohei Fujita<sup>2,3</sup>, Masaaki Hori<sup>4</sup>,  
Koji Kamagata<sup>2</sup>, Shigeki Aoki<sup>2</sup>, Osamu Abe<sup>3</sup>, Hajime Sakamoto<sup>1</sup>,  
Yasuaki Sakano<sup>1</sup>, Shinsuke Kyogoku<sup>1</sup>, and Hiroyuki Daida<sup>1</sup>

**Purpose:** The aim of this study was to investigate whether the detectability of brain volume change in voxel-based morphometry (VBM) with gray matter images is affected by mild white matter lesions (MWLs).

**Methods:** Three-dimensional T<sub>1</sub>-weighted images (3D-T<sub>1</sub>WIs) of 11 healthy subjects were obtained using a 3T MR scanner. We initially created 3D-T<sub>1</sub>WIs with focal cortical atrophy simulated cortical atrophy in left amygdala (type A) and the left medial frontal lobe (type B) from control 3D-T<sub>1</sub>WIs. Next, the following three types of MWL images were created: type A + 1L and type B + 1L images, only one white matter lesion; type A + 4L and type B + 4L images, four white matter lesions at distant positions; and type A + 4L\* and type B + 4L\* images, four white matter lesions at clustered positions. Comparisons between the control group and the other groups were performed with VBM using segmented gray matter images.

**Results:** The gray matter volume was significantly lower in the type A group than in the control group, and similar results were observed in the type A + 1L, type A + 4L, and type A + 4L\* groups. Additionally, the gray matter volume was significantly lower in the type B group than in the control group, and similar results were observed in the type B + 1L, type B + 4L, and type B + 4L\* groups, but the cluster size in type B + 4L\* was smaller than that in type B.

**Conclusion:** Our study showed that the detectability of brain volume change in VBM with gray matter images was not decreased by MWLs as lacunar infarctions. Therefore, we think that group comparisons with VBM should be analyzed by groups including and excluding subjects with MWLs, respectively.

**Keywords:** *diffeomorphic anatomical registration through exponentiated lie algebra, Fazekas classification, lacunar infarction, voxel-based morphometry, white matter lesion*

## Introduction

Voxel-based morphometry (VBM)<sup>1</sup> in three-dimensional T<sub>1</sub>-weighted images (3D-T<sub>1</sub>WIs) obtained via magnetic resonance imaging (MRI) has been used to evaluate the local brain volume change associated with various diseases, such as Alzheimer's disease (AD),<sup>2</sup> idiopathic normal pressure hydrocephalus,<sup>3</sup> epilepsy,<sup>4</sup> diabetes,<sup>5</sup> Parkinson's disease,<sup>6</sup> and panic disorder.<sup>7</sup> VBM is extremely useful for the evaluation of brain

atrophy. In general, subjects with white matter fluid-attenuated inversion recovery (FLAIR) hyperintensities are excluded from VBM studies because white matter FLAIR hyperintensities have been found to be misclassified as gray matter or cerebrospinal fluid (CSF) owing to their intensity characteristics.<sup>8,9</sup> In recent years, VBM, including segmentation repair of tissue misclassification of white matter lesions, has been used in some studies.<sup>10–12</sup> However, this approach requires manual processing, involving manual identification of areas of white matter hyperintensities in native space FLAIR images and segmentation using a space-filling algorithm in ITK-SNAP,<sup>13</sup> which increases the time required when compared with the conventional VBM approach. Moreover, population-specific tissue probability maps (TPMs) were created from images of participants in a study and were used for tissue segmentation with Statistical Parametric Mapping (SPM) 12 software (Wellcome Department of Imaging Neuroscience Group, London, UK; <http://www.fil.ion.ucl.ac.uk/spm>). TPMs are key factors of the results in the tissue segmentation process. If default TPMs implemented in SPM 12 software are used in studies

<sup>1</sup>Department of Radiological Technology, Faculty of Health Science, Juntendo University, Tokyo, Japan

<sup>2</sup>Department of Radiology, Juntendo University School of Medicine, Tokyo, Japan

<sup>3</sup>Department of Radiology, The University of Tokyo Hospital, Tokyo, Japan

<sup>4</sup>Department of Radiology, Toho University Omori Medical Center, Tokyo, Japan

\*Corresponding author: Department of Radiological Technology, Faculty of Health Science, Juntendo University, 2-1-1 Hongo, Bunkyo-ku, Tokyo 113-8421, Japan. Phone: +81-3-3812-1780, Fax: +81-3-3812-1781, E-mail: m.goto@juntendo.ac.jp

©2020 Japanese Society for Magnetic Resonance in Medicine

This work is licensed under a Creative Commons Attribution-NonCommercial-NoDerivatives International License.

Received: October 28, 2019 | Accepted: January 21, 2020

involving VBM, the results can be directly compared. However, if population-specific TPMs are used in studies involving VBM, the results cannot be directly compared. Recently, an automated tool of SPM was provided for detection of FLAIR-hyperintense white-matter lesions.<sup>14</sup> However, the effect of masking of lesions is not clarified in results of VBM.

Diffeomorphic anatomical registration through exponentiated lie algebra (DARTEL) has attracted attention as a group-wise registration algorithm to create templates for spatial normalization in VBM.<sup>15</sup> DARTEL has a stronger ability to deal with local anatomical differences among individuals and can thereby achieve higher registration accuracy than non-DARTEL method.<sup>16</sup> Therefore, even if there is misclassification of white matter lesions, misregistration in spatial normalization to Montreal Neurological Institute (MNI) space is less likely to arise in a normalized gray matter image. We hypothesized that the results of VBM using DARTEL show decreased effect of misclassification in mild white matter lesions (MWLs). Therefore, the present study aimed to investigate whether the detectability of brain volume change in VBM with gray matter images using DARTEL is affected by MWLs.

## Materials and Methods

### Subjects

The study included 11 healthy subjects (eight males, three females; mean age,  $72.8 \pm 3.9$  years; age range, 67–81 years). Subjects were eligible for inclusion if evaluation of their 3D-T<sub>1</sub>WIs and T<sub>2</sub>-weighted images by a board-certified radiologist did not show brain tumors, infarction, hemorrhage, brain atrophy, or white matter lesions graded >1 according to the Fazekas classification.<sup>17</sup> The study protocol was approved by the Institutional Ethics Committee. After explaining the purpose of the study to each subject, written informed consent was obtained from all subjects. To ensure subject confidentiality, data were anonymized.

### MRI scanning protocol

Three-dimensional T<sub>1</sub>-weighted images of the subjects were obtained using a 3T MR scanner (Achieva; Philips Healthcare, Best, The Netherlands) equipped with an eight-channel head coil. Magnetization-prepared rapid gradient-echo imaging was performed to obtain 3D-T<sub>1</sub>WIs, with the following parameters: slice thickness = 0.86 mm, TR/TE = 15/3.4 ms, flip angle = 10°, field of view = 26 × 26 cm, number of excitations = 1, and pixel matrix = 320 × 320. Parallel imaging (sensitivity encoding; SENSE) was performed with a SENSE reduction factor of 2.0. In the present study, these 3D-T<sub>1</sub>WIs are referred to as “control 3D-T<sub>1</sub>WIs.”

### Creating 3D-T<sub>1</sub>WIs with cortical atrophy

We attempted to examine only the influence of MWLs; however, group comparisons (between controls and subjects with cortical atrophy) of clinical images involve other different factors, such as brain shape, brain volume, and image artifacts,

which can affect both groups. Therefore, we created cortical atrophy images that did not include other factors. For all subjects, cortical atrophy images simulated cortical atrophy in left amygdala (type A 3D-T<sub>1</sub>WIs) (Fig. 1) were created by placing spherical regions of interest (ROI) having a 6-mm diameter (6 mm-ROI) on the left amygdala in control 3D-T<sub>1</sub>WIs using Multi-image Analysis GUI (Mango) software (University of Texas Health Science Center, San Antonio, TX, USA; <https://www.nitrc.org/projects/mango>). Additionally, the 6 mm-ROI is used in “Creating 3D-T<sub>1</sub>WIs with MWLs”. ROI must be set inside the area of white matter and must not invade gray matter and CSF. If ROI bigger than the 6 mm-ROI was used, it was difficult to set ROI inside the area of white matter. The signal intensity inside each ROI was changed to that of CSF. Signal intensities of CSF were measured in the area nearest to the individual ROI. Moreover, other cortical atrophy images were created to examine the effect of the geometrical distance between the region of atrophy and the white matter lesion. These cortical atrophy images (type B 3D-T<sub>1</sub>WIs) (Fig. 2) were created by placing ROI on the left medial frontal lobe in control 3D-T<sub>1</sub>WIs using Mango software. The signal intensity inside each ROI was changed to that of CSF. Signal intensities of CSF were measured in the area nearest to the individual ROI. Briefly, we prepared Type A (cortical atrophy in left amygdala), Type B (cortical atrophy in medial frontal lobe), and control 3D-T<sub>1</sub>WIs.

### Creating 3D-T<sub>1</sub>WIs with MWLs

For all subjects, 6 mm-ROI was carefully placed on white matter in type A and type B 3D-T<sub>1</sub>WIs using Mango software, and the signal intensity inside each ROI was changed to that of gray matter. Signal intensities of gray matter were measured in the area nearest to the individual ROI. Type A 3D-T<sub>1</sub>WIs with a white matter lesion (type A + 1L) and type B 3D-T<sub>1</sub>WIs with a white matter lesion (type B + 1L) are shown in Figs. 1 and 2, respectively. In these images, 6 mm-ROI was carefully placed on the left side of frontal white matter. Type A 3D-T<sub>1</sub>WIs with four white matter lesions (type A + 4L) and type B 3D-T<sub>1</sub>WIs with four white matter lesions (type B + 4L) are shown in Figs. 1 and 2, respectively. In these images, 6 mm-ROIs were carefully placed on both sides of frontal and occipital white matter. Additionally, type A 3D-T<sub>1</sub>WIs with four white matter lesions (type A + 4L\*) and type B 3D-T<sub>1</sub>WIs with four white matter lesions (type B + 4L\*) are shown in Figs. 1 and 2, respectively. In these images, 6 mm-ROIs were carefully set on white matter near the atrophic regions in type B images. Distance between atrophic region and MWLs is long in type A + 4L\* compared with that in type B + 4L\*. Results with these T<sub>1</sub>WI show the effect of distance between atrophic region and MWLs.

### Image preprocessing for group comparisons with VBM

All 3D-T<sub>1</sub>WIs (11 control, 11 type A, 11 type B, 11 type A + 1L, 11 type B + 1L, 11 type A + 4L, 11 type B + 4L, 11 type A + 4L\*, and 11 type B + 4L\* 3D-T<sub>1</sub>WIs) were analyzed using

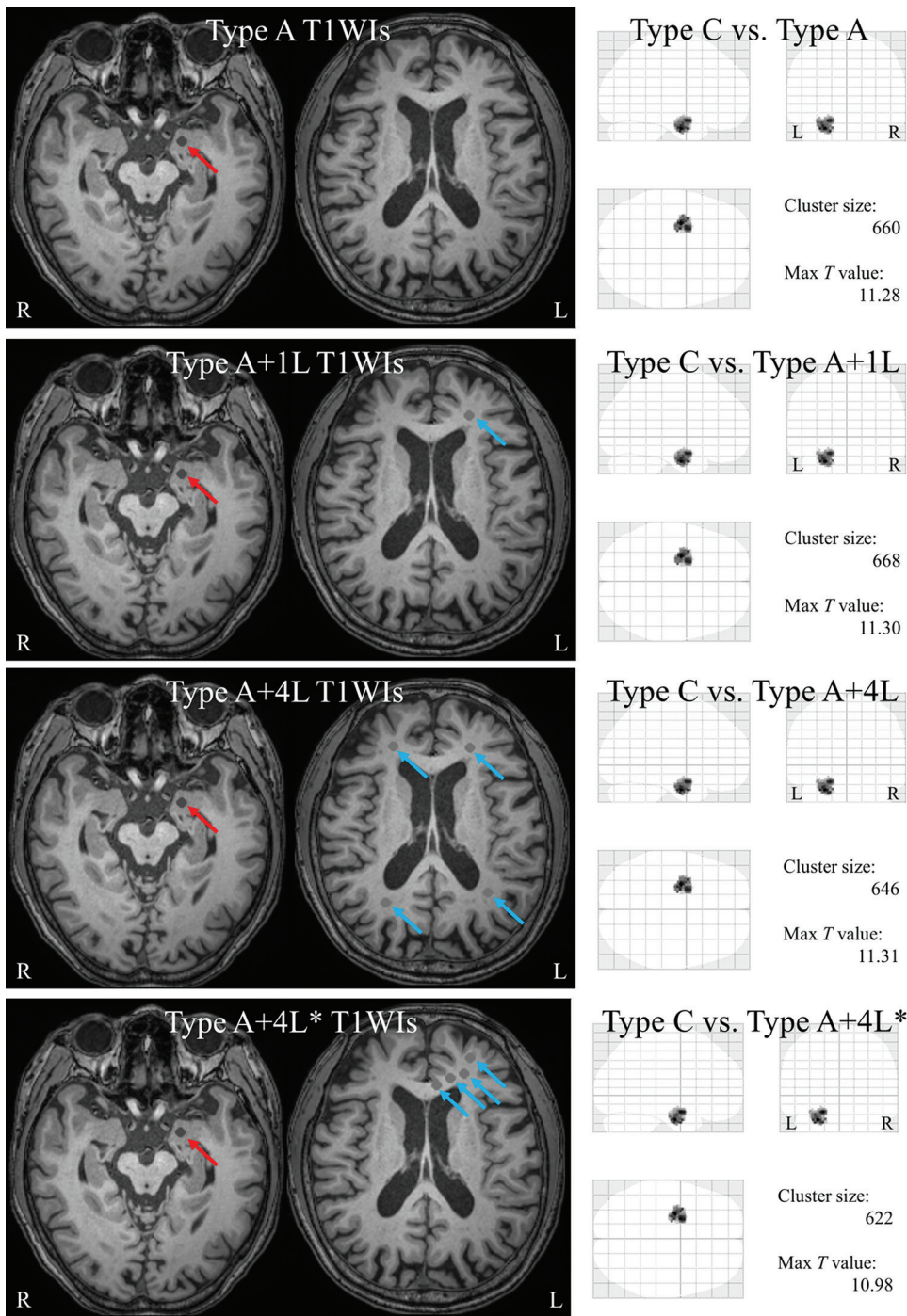


**Fig. 1** The left column includes type A T<sub>1</sub>WIs (slice levels are the amygdala and mild white matter lesions) in the first row, type A + 1L T<sub>1</sub>WIs in the second row, type A + 4L T<sub>1</sub>WIs in the third row, and type A + 4L\* T<sub>1</sub>WIs in the fourth row. Type A is indicated by cortical atrophy images of left amygdala. Red arrows show atrophy lesions, whereas blue arrows show mild white matter lesions. The figures in the right column indicate all regions in which the gray matter volume is significantly lower in the type A, type A + 1L, type A + 4L, and type A + 4L\* groups than in the control group, using a gray scale. A  $P$ -value  $< 0.001$  (uncorrected in voxel-wise difference, cluster size of  $\geq \text{FDRc}$  in table of SPM results) is considered statistically significant. The cluster size indicates voxel numbers with a significant difference in gray matter volume between groups.

SPM 12 software. During segmentation, the affine regularization space template from the International Consortium for Brain Mapping was changed from European to East Asian because all subjects were Japanese, whereas default settings were used for all other parameters. Additionally, DARTEL-imported data of control 3D-T<sub>1</sub>WIs were saved for creation of DARTEL templates.

Segmented gray matter images in native space were normalized into the MNI template space using DARTEL methods,<sup>15</sup> individually. In the normalization, DARTEL

templates with control were used for all 3D-T<sub>1</sub>WIs. Intensity was modulated and smoothed with 8 mm full-width at half-maximum Gaussian kernel.

#### **Statistical analyses for group comparisons with VBM**

The paired  $t$ -test was used for comparisons between the control group and the other groups (i.e., control vs. type A, control vs. type A + 1L, control vs. type A + 4L, control vs. type A + 4L\*, control vs. type B, control vs. type B + 1L, control vs. type B + 4L, and control vs. type B + 4L\*) with VBM using SPM 12

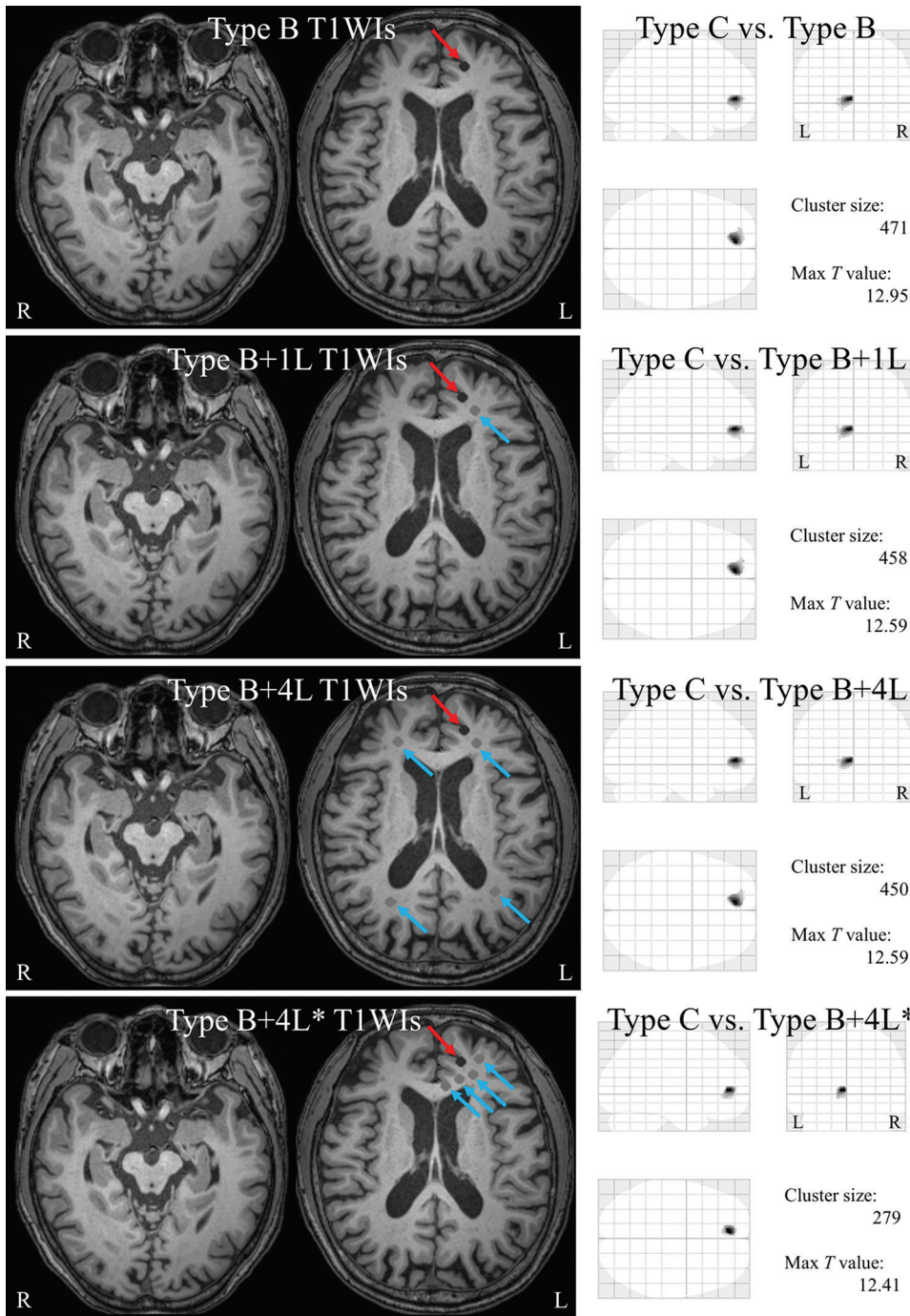


**Fig. 2** The left column includes type B T<sub>1</sub>WIs (slice levels are the amygdala and mild white matter lesions) in the first row, type B + 1L T<sub>1</sub>WIs in the second row, type B + 4L T<sub>1</sub>WIs in the third row, and type B + 4L\* T<sub>1</sub>WIs in the fourth row. Type B is indicated by cortical atrophy images of left medial frontal lobe. Red arrows show atrophy lesions, whereas blue arrows show mild white matter lesions. The figures in the right column indicate all regions in which the gray matter volume is significantly lower in the type B, type B + 1L, type B + 4L, and type B + 4L\* T<sub>1</sub>WIs in the gray matter volume than in the control group, using a gray scale. A *P*-value <0.001 (uncorrected in voxel-wise difference, cluster size of ≥FDR<sub>c</sub> in table of SPM results) is considered statistically significant. The cluster size indicates voxel numbers with a significant difference in gray matter volume between groups.

software. In the group comparisons, a *P*-value <0.001 (uncorrected in voxel-wise difference, cluster size of ≥ FDR<sub>c</sub> in table of SPM results) was considered statistically significant.

## Results

The right columns in Figs. 1 and 2 show the regions with decreased gray matter volume in each type group when compared with the finding in the control group in VBM, and a summary is shown in Table 1. Increased gray matter volumes

in some results with VBM were observed at not only near MWL but also the far regions.

The first row in Fig. 1 shows all the regions in which the gray matter volume was significantly lower in the type A group than in the control group. The MNI coordinates of the local maxima were -27, -8, and -30 (uncorrected *P* < 0.0001, *T* = 11.28, cluster size = 660). The second row in Fig. 1 shows all the regions in which the gray matter volume was significantly lower in the type A + 1L group than in the control group. The MNI coordinates of the local maxima were

**Table 1** Summary of paired *t*-test results in voxel-based morphometry

	Cluster size	Max <i>T</i> -value	MNI coordinates
Control vs. Type A	660	11.28	-27, -8, -30
Control vs. Type A + 1L	668	11.30	-27, -8, -30
Control vs. Type A + 4L	646	11.31	-27, -8, -30
Control vs. Type A + 4L*	622	10.98	-27, -8, -30
Control vs. Type B	471	12.95	-6, -47, 3
Control vs. Type B + 1L	458	12.59	-6, -47, 3
Control vs. Type B + 4L	450	12.59	-6, -47, 3
Control vs. Type B + 4L*	279	12.41	-6, -47, 3

The cluster shows decreased gray matter volume in each type group when compared with the finding in the control group. The cluster size indicates voxel numbers with a significant difference in gray matter volume between groups. The MNI coordinates are the Montreal Neurological Institute coordinates of local maxima. A *P*-value <0.001 (uncorrected in voxel-wise difference, cluster size of  $\geq$ FDRc in table of SPM results) was considered statistically significant.

-27, -8, and -30 ( $P < 0.0001$ ,  $T = 11.30$ , cluster size = 668). The third row in Fig. 1 shows all the regions in which the gray matter volume was significantly lower in the type

A + 4L group than in the control group. The MNI coordinates of the local maxima were -27, -8, and -30 ( $P < 0.0001$ ,  $T = 11.31$ , cluster size = 646). The fourth row in Fig. 1 shows all the regions in which the gray matter volume was significantly lower in the type A + 4L\* group than in the control group. The MNI coordinates of the local maxima were -27, -8, and -30 ( $P < 0.0001$ ,  $T = 10.98$ , cluster size = 622).

The first row in Fig. 2 shows all the regions in which the gray matter volume was significantly lower in the type B group than in the control group. The MNI coordinates of the local maxima were -6, -47, and 3 ( $P < 0.0001$ ,  $T = 12.95$ , cluster size = 471). The second row in Fig. 2 shows all the regions in which the gray matter volume was significantly lower in the type B + 1L group than in the control group. The MNI coordinates of the local maxima were -6, -47, and 3 ( $P < 0.0001$ ,  $T = 12.59$ , cluster size = 458). The third row in Fig. 2 shows all the regions in which the gray matter volume was significantly lower in the type B + 4L group than in the control group. The MNI coordinates of the local maxima were -6, -47, and 3 ( $P < 0.0001$ ,  $T = 12.59$ , cluster size = 450). The fourth row in Fig. 2 shows all the regions in which the gray matter volume was significantly lower in the type B + 4L\* group than in the control group. The MNI coordinates of the local maxima were -6, -47, and 3 ( $P < 0.0001$ ,  $T = 12.41$ , cluster size = 279). Figure 3 shows an example segmented images in a subject of type B + 4L\*.

## Discussion

The present study found that the detectability of brain volume change in VBM with gray matter images was not decreased by MWLs as lacunar infarctions.

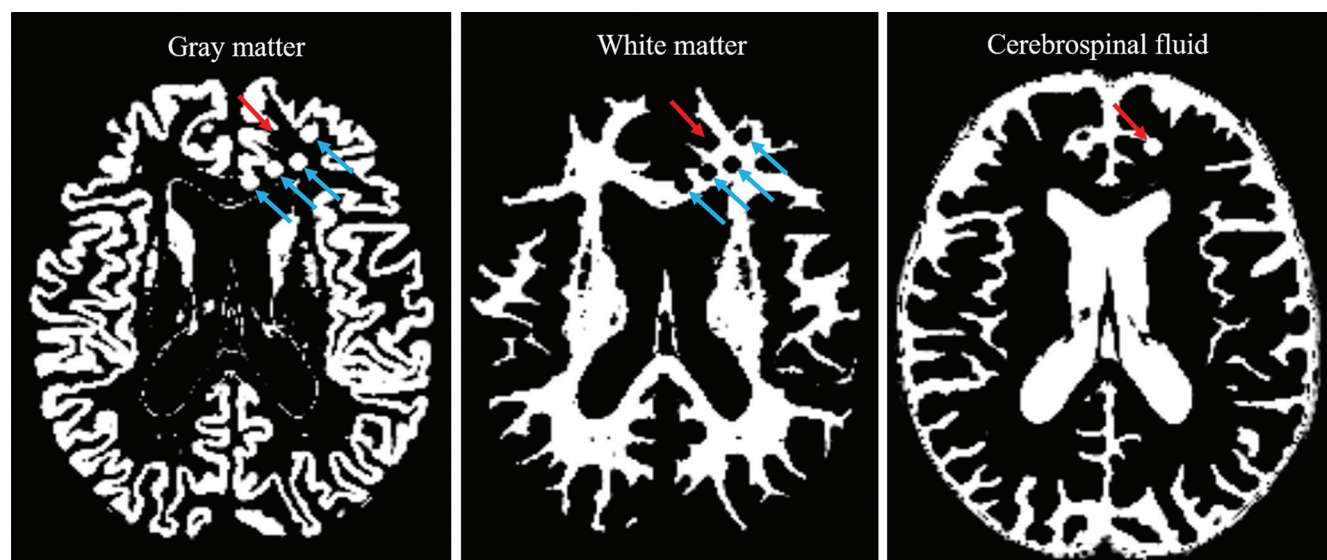


**Fig. 3** Segmented images in a subject of type B + 4L\*. Red arrows show cortical atrophy lesions, whereas blue arrows show mild white matter lesions. The region as atrophy was segmented as cerebrospinal fluid and not as gray matter, and the regions as mild white matter lesion were segmented as gray matter and not as white matter.

We attempted to examine only the influence of MWLs, but group comparisons (between controls and subjects with cortical atrophy) of clinical images involve other different factors, such as brain shape, brain volume, and image artifacts, which can affect both groups. There, we created cortical atrophy images that did not include other factors. Especially, a motion artifact is one of the major causes of misclassification. Motion artifacts result in signal intensity changes in  $T_1$ WIs. A region with decreased signal intensity in white matter might be segmented as gray matter, whereas a region with increased signal intensity in gray matter might be segmented as white matter. Thus, the amount of misclassification differs among motion artifacts in subjects.

With regard to control vs. type A and control vs. type B comparisons, significantly decreased gray matter volumes were detected near the 6 mm-ROI in type A and type B  $T_1$ WIs. The region inside the 6 mm-ROI was segmented as CSF and not as gray matter, because the signal intensity inside the ROI was the same as that of CSF. Therefore, type A and type B  $T_1$ WIs are an appropriate images as cortical atrophy model.

We created type A and type B 3D- $T_1$ WIs with a white matter lesion (type A + 1L and type B + 1L, respectively). The VBM result for control vs. type A + 1L (cluster size: 668, max  $T$ -value: 11.30) was extremely close to the result for control vs. type A (cluster size: 660, max  $T$ -value: 11.28). Moreover, the VBM result for control vs. type B + 1L (cluster size: 458, max  $T$ -value: 12.59) was extremely close to the result for control vs. type B (cluster size: 471, max  $T$ -value: 12.95). The cluster size ratio (cluster size with a white matter lesion/cluster size without a white matter lesion) for type B + 1L and type B images was lower than that for type A + 1L and type A images. Additionally, the distance between atrophy and the white matter lesion in type B + 1L images was shorter than that in type A + 1L images. Almost all white matter lesions were segmented to gray matter and not white matter. In gray matter images of type B + 1L, the distance between atrophy and the region of misclassification was extremely short. Therefore, we consider that the degree of registration in spatial normalization with DARTEL in SPM 12 software was influenced by the distance between atrophy and the white matter lesion.

We created 3D- $T_1$ WIs with three white matter lesions added to type A + 1L and type B + 1L (type A + 4L and type B + 4L, respectively). The differences between the groups with one white matter lesion and the groups with four white matter lesions were extremely small as follows: cluster size 668/646 and max  $T$ -value 11.30/11.31 for control vs. type A + 1L/type A + 4L, and cluster size 458/450 and max  $T$ -value 12.59/12.59 for control vs. type B + 1L/type B + 4L. These results indicate that white matter lesions (grade 2 according to the Fazekas classification) did not affect the results in VBM with gray matter images. In our study, the 6 mm-ROIs were used to simulate MWL. We hypothesized that the effect on significant cluster size in atrophy increases by using bigger ROI compared with the 6 mm-ROI. Therefore, we used not only  $T_1$ WI with single MWL but also  $T_1$ WI with 4L (four MWLs).

In the final examination, we set four white matter lesions near the left medial frontal lobe. The cluster size decreased to 279 for control vs. type B + 4L\* when compared with 471 for control vs. type B. The cluster size for control vs. type B + 4L\* was smaller than that for control vs. type A + 4L\* because the distance between atrophy and the four white matter lesions was much shorter in type B + 4L\* images than in type A + 4L\* images. Thus, if gray matter volume reduction in VBM exists far from a white matter lesion graded as 2 according to the Fazekas classification, the reduction might reflect true volume change. However, we did not use images of subjects with white matter lesions graded as 2 because white matter lesions have various signal intensities. The profile curve of signal intensity in analyzed  $T_1$ WIs is a key factor in the segmentation process with SPM 12 software.<sup>18,19</sup> In the present study, segmented gray matter images included most MWLs because the signal intensity of white matter lesions was set to the signal intensity of gray matter.

In general, subjects with white matter hyperintensities are excluded from VBM studies. Previous studies have used the following various exclusion criteria: “focal brain lesions, such as tumors and infarcts in MRI images”,<sup>20</sup> “anatomical abnormalities”,<sup>21</sup> “visible white matter hyperintensities (Fazekas grade 2 or higher)”,<sup>22</sup> “more than three subcortical white matter hyperintensities exceeding 10 mm in diameter as examined on  $T_2$ -weighted MRI”,<sup>23</sup> and “vascular lesions visible in structural images”.<sup>24</sup> MWLs are segmented to gray matter or CSF. If the signal intensity of an MWL is near that of gray matter, the MWL is segmented as gray matter. In addition, the tissue probability of gray matter in MWL was increased by decreased distance between an MWL and gray matter. Information in segmented gray and white matter images were used in spatial normalization. The effect of misclassification in group comparison with VBM is increased by using MWL with signal intensity of gray matter, compared with MWL with signal intensity of CSF. Therefore, we changed signal intensity inside MWL to that of gray matter, not CSF. In our results, some MWLs were segmented to CSF, not gray matter. In this case, some MWLs were placed near the lateral ventricle compared with other MWLs. If the signal intensity of MWL inside an ROI is changed to that of CSF, most MWLs were segmented to CSF.

A major limitation of the present study is that we examined only the influence of MWLs. VBM involving clinical images includes the influences of image distortion, signal intensity uniformity, misregistration in the spatial normalization process, modulation effect, brain tissue degeneration, change in image contrast, and image artifacts.<sup>3,16,18,19,25-27</sup> The second limitation is that our study was unable to define a clear inclusion criteria for subjects with MWLs because serious decrease of significant cluster size was found in the control vs. type B + 4L\*, but not in the control vs. type A + 4L\*. In the clinical setting, effect of MWLs may decrease compared with our results because positions of MWLs may vary in individuals. The detectability of brain atrophy with VBM may be

further improved on including patients with MWLs because the presence of a large number of subjects increases the power of statistical analyses. Therefore, we think that group comparisons with VBM should be analyzed by groups including and excluding subjects with MWLs, respectively.

## Conclusion

Our study showed that the detectability of brain volume change in VBM with gray matter images was not decreased by MWLs as lacunar infarctions. Many previous studies involving VBM excluded subjects with white matter lesions (grade >1 according to the Fazekas classification). We think that group comparisons with VBM should be analyzed by groups including and excluding subjects with MWLs, respectively.

## Conflicts of Interest

The authors declare that they have no conflicts of interest.

## References

- Ashburner J, Friston KJ. Voxel-based morphometry—the methods. *Neuroimage* 2000; 11:805–821.
- Matsuda H, Mizumura S, Nemoto K, et al. Automatic voxel-based morphometry of structural MRI by SPM8 plus diffeomorphic anatomic registration through exponentiated lie algebra improves the diagnosis of probable Alzheimer Disease. *AJNR Am J Neuroradiol* 2012; 33:1109–1114.
- Goto M, Abe O, Aoki S, et al. Combining segmented grey and white matter images improves voxel-based morphometry for the case of dilated lateral ventricles. *Magn Reson Med Sci* 2018; 17:293–300.
- Keller SS, Roberts N. Voxel-based morphometry of temporal lobe epilepsy: an introduction and review of the literature. *Epilepsia* 2008; 49:741–757.
- Musen G, Lyoo IK, Sparks CR, et al. Effects of type 1 diabetes on gray matter density as measured by voxel-based morphometry. *Diabetes* 2006; 55:326–333.
- Goto M, Kamagata K, Hatano T, et al. Depressive symptoms in Parkinson's disease are related to decreased left hippocampal volume: correlation with the 15-item shortened version of the Geriatric Depression Scale. *Acta Radiol* 2018; 59:341–345.
- Hayano F, Nakamura M, Asami T, et al. Smaller amygdala is associated with anxiety in patients with panic disorder. *Psychiatry Clin Neurosci* 2009; 63:266–276.
- Grau-Olivares M, Bartrés-Faz D, Arboix A, et al. Mild cognitive impairment after lacunar infarction: voxel-based morphometry and neuropsychological assessment. *Cerebrovasc Dis* 2007; 23:353–361.
- Goto M, Abe O, Miyati T, et al. 3 Tesla MRI detects accelerated hippocampal volume reduction in postmenopausal women. *J Magn Reson Imaging* 2011; 33:48–53.
- Benjamin P, Lawrence AJ, Lambert C, et al. Strategic lacunes and their relationship to cognitive impairment in cerebral small vessel disease. *Neuroimage Clin* 2014; 4:828–837.
- Lambert C, Zeestraten E, Williams O, et al. Identifying preclinical vascular dementia in symptomatic small vessel disease using MRI. *Neuroimage Clin* 2018; 19:925–938.
- Lambert C, Sam Narean J, Benjamin P, Zeestraten E, Barrick TR, Markus HS. Characterising the grey matter correlates of leukoaraiosis in cerebral small vessel disease. *Neuroimage Clin* 2015; 9:194–205.
- Yushkevich PA, Piven J, Hazlett HC, et al. User-guided 3D active contour segmentation of anatomical structures: significantly improved efficiency and reliability. *Neuroimage* 2006; 31:1116–1128.
- Schmidt P, Gaser C, Arsic M, et al. An automated tool for detection of FLAIR-hyperintense white-matter lesions in Multiple Sclerosis. *Neuroimage* 2012; 59:3774–3783.
- Ashburner J. A fast diffeomorphic image registration algorithm. *Neuroimage* 2007; 38:95–113.
- Goto M, Abe O, Aoki S, et al. Diffeomorphic Anatomical Registration Through Exponentiated Lie Algebra provides reduced effect of scanner for cortex volumetry with atlas-based method in healthy subjects. *Neuroradiology* 2013; 55:869–875.
- Fazekas F, Chawluk JB, Alavi A, Hurtig HI, Zimmerman RA. MR signal abnormalities at 1.5 T in Alzheimer's dementia and normal aging. *AJR Am J Roentgenol* 1987; 149:351–356.
- Goto M, Abe O, Miyati T, et al. Influence of signal intensity non-uniformity on brain volumetry using an atlas-based method. *Korean J Radiol* 2012; 13:391–402.
- Goto M, Yamashita F, Kawaguchi A, et al. The effect of single-scan and scan-pair intensity inhomogeneity correction methods on repeatability of voxel-based morphometry with multiple magnetic resonance scanners. *J Comput Assist Tomogr* 2018; 42:111–116.
- Yamashita F, Sasaki M, Saito M, et al. Voxel-based morphometry of disproportionate cerebrospinal fluid space distribution for the differential diagnosis of idiopathic normal pressure hydrocephalus. *J Neuroimaging* 2014; 24:359–365.
- Karavasilis E, Parthimos TP, Papatriantafyllou JD, et al. A specific pattern of gray matter atrophy in Alzheimer's disease with depression. *J Neurol* 2017; 264:2101–2109.
- Guo X, Wang Z, Li K, et al. Voxel-based assessment of gray and white matter volumes in Alzheimer's disease. *Neurosci Lett* 2010; 468:146–150.
- Sydykova D, Stahl R, Dietrich O, et al. Fiber connections between the cerebral cortex and the corpus callosum in Alzheimer's disease: a diffusion tensor imaging and voxel-based morphometry study. *Cereb Cortex* 2007; 17:2276–2282.
- Li X, Messé A, Marrelec G, Péligrini-Issac M, Benali H. An enhanced voxel-based morphometry method to investigate structural changes: application to Alzheimer's disease. *Neuroradiology* 2010; 52:203–213.
- Goto M, Abe O, Kabasawa H, et al. Effects of image distortion correction on voxel-based morphometry. *Magn Reson Med Sci* 2012; 11:27–34.
- Goto M, Abe O, Miyati T, Yamasue H, Gomi T, Takeda T. Head motion and correction methods in resting-state functional MRI. *Magn Reson Med Sci* 2016; 15:178–186.
- Goto M, Abe O, Miyati T, Aoki S, Gomi T, Takeda T. Mis-segmentation in voxel-based morphometry due to a signal intensity change in the putamen. *Radiol Phys Technol* 2017; 10:515–524.